Thesis

Defect Chaos in Electro-Hydrodynamic Convection
of
Nematic Liquid Crystals

Shin-ichi Sasa

Department of Physics, Kyoto University

ABSTRACT

We present and study simple mathematical models which exhibit a transition from stationary periodic patterns to defect chaos in electro-hydrodynamic convection of nematic liquid crystals. A nonlinear phase equation is derived from our models, whose method follows the Cross-Newell theory. The stability analysis of normal rolls and weakly nonlinear analysis near the phase instability are developed on the basis of the phase equation. Pattern evolution and statistical properties in the regime of defect chaos are also discussed with the aid of numerical simulations of a computationally efficient model which we worked out.

Acknowledgment

Contents

1.Introduction

Let us consider a two-dimensional system in which spatial periodic patterns are formed. These systems often exhibit weakly disordered structures such as topological defects i.e. the point singularities in the phase fields associated with the periodic patterns. In the first stage of the ordering process, the periodic patterns are locally formed and a defect appears at the point connecting two periodic patterns with identical orientation but slightly different wavelengths. Since defects are topologically stable in two-dimensional systems [1], the motion of a defect is well-defined until it vanishes on collision with an anti-defect i.e. the defect with an opposite topological number. Therefore, defects should play important roles in the late stage of ordering process [2-9]. On the other hand, defects can also be created spontaneously through the instability of periodic patterns. In that case, if unstable periodic patterns are reorganized after the defect creation, the system still retains its unstable nature, and such a state is called *defect chaos* or *defect turbulence*. Since defect chaos has weakly disordered spatial structures, this may be classified into *weak turbulence* rather than *developed turbulence*[10].

Defect chaos seems to be a new mode of motion. We therefore try to clarify the nature of defect chaos by exploring the following specific problems:

(1) Finding scenarios for the transition to defect chaos.

(2) Describing the pattern dynamics.

(3) Characterizing statistical properties of defect chaos.

It would be necessary to approach these problems both experimentally and theoretically. When a theorist tries to solve a problem, he needs a model which has both quantitative predictability and practical computability.

Recently, the complex Ginzburg-Landau equation has been studied by Coullet et al.[11,12] as a model for defect turbulence. This model equation describes the behavior near the *Hopf bifurcation* [13-16], and the defect is then defined as a singularity of *temporal phase* or *propagative phase*[17,18]. However, the non-linear interactions and destabilization of *waves* emitted from the defects are important ingredients of the dynamics in this kind of oscillatory medium[19], so that its

behavior should be rather different and more complex as compared to that of non-oscillating systems which is of our main concern. A coupled-map-lattice (CML) approach, which was first proposed by Kaneko, also gives a useful model for studying spatio-temporal chaos, and several essential features of transition and statistical properties were exhibited[20-22]. However, it is difficult to know what physical processes are expressed by CML, that is, the correspondence between CMLs and real phenomena remains quite abstract and indirect.

As implied above, theoretical research for defect chaos remains poor for the lack of a suitable model. On the contrary, experimental works were developed to a considerable extent by working with electro-hydrodynamic convections (EHC) of nematic liquid crystals (NLC)[23-31].

Nematic liquid crystals, which consist of elongated molecules, are a fluid with an orientational order described by the director. They have thus anisotropic properties whether they are in or out of thermal equilibrium, and show a rich variety of patterns when A.C. electric fields are applied, as systematically studied by Kai and his coworker[24]. Let us sketch the system behavior near the onset of convection. On increasing the voltage in the conduction regime below a critical frequency, a stationary roll pattern appears with a preferred direction due to the anisotropy[32-34]. If the preferred direction of the rolls is normal (or oblique) to the direction of the directors, the rolls are called *normal rolls (or oblique rolls)*, and the normal rolls are also called the Williams domains (WD)[28]. Which type of the rolls appears depends on the frequency; for example, the normal rolls are formed beyond a frequency called the Lifshitz point. Increasing the voltage further in the normal roll regime, one finds a secondary bifurcation to the fluctuating Williams domain (FWD), as named by Kai[23]. In this regime, where the basic roll structure is still retained, a dynamic steady state is maintained through the creations and annihilations of defects. FWD is nothing but defect chaos. We thus wish to investigate the nature of FWD theoretically.

First of all, we must consider which model is the best fitted to our present study. Although the study based on the microscopic models may make quan-

titative predictions, some of them do not satisfy the computability condition mentioned before. Indeed, in EHC, it is difficult to treat such basic equations in EHC analytically or numerically[35]. Thus, one of the main purposes in the present paper is to construct a suitable model for defect chaos in EHC of NLC.

Since defect chaos appears on a macroscopic scale, we want to express it with a macroscopic description which is suitable also for the description of roll patterns. Our approahes are twofolds. One is called the method of the amplitude equation which is mathematically justified. If we are concerned with the regime near the onset of convections, it would be possible to simplify the dynamics into the dynamics of the amplitude of the critical mode[36,37]. Though the amplitude equation in EHC was derived by Bodenschatz et al.[38], it can never describe the transition between WD and FWD. This implies that some higher order terms become essential beyond a finite distance apart from the onset of convection. One may therefore expect that the transition to defect chaos could be described by taking account of such terms. Actually, however, it is very difficult to calculate higher order terms, and the method of the amplitude equation does not seem to appropriate for describing defect chaos.

Another approach is a phenomenological one in which some important effects are heuristically taken into the equation. In that approach, we can predict no quantitative details but we are only concerned with universal features of the phenomena. How to construct a phenomenological model equation is the following. We first study experimental facts about the onset of convections and try to know the type of bifurcation by checking the continuity of transitions, onset frequency and codimension. It is known that the transition to WD occurs through a supercritical stationary bifurcation. Second, we take account of some invariance properties to be require under the transformations such as translation, reflection, rotation and the Galilei transformations. A model in EHC should satisfy the first two symmetries. Finally, some simplicity of the model should be demanded; for example, the order of the spatial derivatives or dynamical variables which appears in the model should not be too high. However, too simplified models could

not capture the phenomena, and therefore it is not always easy to require simplicity from a certain guiding principle. Such difficulty makes contrast with the case of the amplitude equation method for which a simple form can be obtained by the scaling hypothesis. We must thus make trial and error until we obtain a reasonable model. Unfortunately, a simple model for EHC which was presented by Pesch and Kramer can not exhibit the transition to defect chaos although their model equation can explain some behaviors such as the normal roll-oblique roll transition.[39] We must thus extend their model so that it may describe efect chaos. In section 2, we will present the Pesch-Kramer model supplemented with drift terms[40], and the equation for the drift field which is induced by the deformations of rolls will be determined by the requirements of the symmetries and simplicity.

The importance of drift effects was first pointed out by Siggia and Zippelius[41,42]. In the systems under stress free boundary conditions, a large scale horizontal flow (drift) becomes a relevant dynamical variable because the Galilei symmetry must be satisfied by the system. On the other hand, Cross showed that skewed varicose instability is caused by the drift effects under rigid boundary conditions[43]. This fact is somewhat mysterious because the drift flow is not a relevant dynamical variable in the case of rigid boundary conditions. In this case, however, the drift effects play two roles. First, the drift terms produce nonlinear terms including higher order spatial derivatives. Second, the same effects cause nonlocality because the pressure field in a incompressible fluid is nonlocally determined and the drift flows have a part coming from the pressure gradient. As we will argue in section 5, skewed varicose instability occurs as a results of this nonlocality[43,44].

We now introduce the analysis based on our own models. A necessary condition for the appearance of defect chaos is that the normal rolls become unstable at a finite distance apart from the convection onset. In that case, the type of instability should be a long wavelength instability (phase instability) because *the local order* must be retained. Then, one may ask whether or not the phase

gradient remains bounded when the phase instability occurs. If the phase gradient remains bounded and exhibits chaotic behaviors, then this state may be called *phase turbulence* whose notion was first proposed by Kuramoto[45]. We notice that phase turbulence appears only when the temporal symmetry breaks down. As other possibilities, phase deformation may lead to a stable pattern, or otherwise amplitude deformation may be caused leading to spontaneous creation of defects. In order to understand such behaviors, we must make a weakly non-linear analysis.

Phase dynamics which describes the deformations of rolls is a powerful tool for studying these problems: it not only gives the descriptions of the slow relaxation to a stable state, but also determines the marginal stability lines on which the phase instability takes place[46]. Although the standard phase dynamics does not describe the behavior beyond the marginal stability lines, Kuramoto improved it by developing a weakly nonlinear analysis for phase instabilities[47].

In section 3, we will derive the phase dynamics for our model equations following the Cross-Newell approach[44]. In section 4, we will argue the linear stability analysis of normal rolls based on the linearized phase equation. We will classify the types of the phase instability by specifying the most unstable mode, as was done by Busse for the Rayleigh-Bénard convections[48,49], and determine which type of instability leads to defect chaos. In section 5, a nonlinear phase equation will be derived from a weakly nonlinear analysis, and we will argue the behavior beyond the phase instability with the use of this equation.

Discussions based only on the stability analysis can not give a definite answer to the question whether or not our models serve as suitable models for defect chaos. We are thus led to their numerical simulations. In computer simulations of PDE, however, we always have the question of reliability. On the other hand, we have also models such as celluar automata[50] and CMLs which are free from such problems. These models are more suitable to treat numerically; their simulations may be looked upon as those of the real phenomena themselves. Such a view was advanced strongly by Oono and Puri in their paper: They say *"Nature gives*

physicist phenomena, not equation"[51,52]. If we are concerned with universal macroscopic properties which are independent of microscopic details, we prefer to simulate a computationally efficient model. It would therefore be an important step in our theory to construct such a CML model that could describe the same universal behavior as a PDE model does. The problem of constructing a best CML is quite difficult to solve in general. Still, Oono and Puri presented a method to construct a CML model corresponding to a PDE model in spinodal decomposition problems[51,52]. Although their method has never been justified mathematically, it is expected to apply to many other problems.

In section 6, we will present a CML version of our model and carry out its numerical simulations so that we may study pattern evolution and statistical properties. We will focus on the temporal variations of the number of defects, because the term *defect chaos* comes from their chaotic variations, implying the importance of investigating their statistical properties[27,30]. In the final section, a few additional comments will be given.

2. Phenomenological Models

A typical example of phenomelogical equations in convective systems is the Swift-Hohenberg equation which was derived from the Boussinesq equation under some approximations[53]. Let us explain their model equation. Consider the situation that steady periodic rolls are super-critically formed in an isotropic system. Let the vertical velocity be denoted by w. Then, the form of the equation for w is constrained by the following two requirements. First, the equation must exhibit a super-critical steady bifurcation at $R = R_c$ and the critical wavenumber k_c must be finite. Second, the equation must satisfy the Euclid symmetry and be invariant under the transformation $w \rightarrow -w$. We further require the simplicity such that the heighest order of the spatial derivatives should be minimal. Then the model equation takes the form:

$$\dot{w} = Rw - w^3 - (1 + \Delta)^2 w, \tag{2.1}$$

where $\Delta = \partial_x^2 + \partial_y^2$ and R is a control parameter which corresponds to the temperature gradient.

This model equation has a potential such that the system relaxes to one of its minima. Since the minima of the potential are degenerate due to the rotational symmetry involved, its relaxational dynamics has a very long time scale and the system often relaxes to non-trivial steady patterns with grain boundaries by the influence of latenal boundaries. Detailed simulations of this model equation which were performed by Greenside and Coughran also show such behavior [54].

There are some variants of the Swift-Hohenberg equation[39,55-58]. In particular, Pesch and Kramer presented as a phenomenological model of EHC an anisotropic version of the Swift-Hohenberg equation[39]:

$$\dot{w} = Rw - w^3 + \hat{D}w,$$
$$\hat{D} = -(1 + \Delta)^2 - \eta_1 \partial_y^4 - 2\eta_2 \partial_x^2 \partial_y^2. \tag{2.2}$$

Here η_1 and η_2 are anisotropic parameters, and R is a control parameter corresponding to the voltage of the applied electric field. This model equation is the

simplest model of those taking account of the anisotropy. We now review the behavior of this model equation near the onset of convections[39].

Without external forces, the fluid remains in a rest state $w = 0$. When A.C. electric fields are applied and the voltage reaches a critical value, convections set in. This fact implies that the rest state $w = 0$ becomes unstable against the disturbance with non-zero wavevector. We thus analyse the linear stability of the rest state. Denoting the growth rate of the disturbance around the uniform state $w = 0$ by λ, we obtain from the model equation eq.(2.2)

$$
\begin{aligned}
\lambda(k, \varphi) &= R - (k^2 - 1)^2 - \eta_1 k^4 \sin^4 \varphi - 2\eta_2 k^4 \sin^2 \varphi \cos^2 \varphi, \\
&= R - 1 + 2k^2 - k^4 (1 + 2\eta_2 \sin^2 \varphi + (\eta_1 - 2\eta_2) \sin^4 \varphi)
\end{aligned}
\tag{2.3}
$$

where $\vec{k} = (k \cos \varphi, k \sin \varphi)$ $(k \geq 0)$ is the wavevector of the disturbance. Consider the situations in which the directors in the rest state are aligned in the x-direction. Then, the growth of disturbances in the y-direction is inhibited. This fact is explained by the condition $\eta_1 > 0$, and we will assume this condition below. The critical wavevector $\vec{k}_c$ and the control parameter R_c at which the convections occur are determined from the condition that the maximum value of λ becomes positive. The magnitude of the critical wavevector should be finite or zero so that the system may remain stable. Therefore, for arbitrary φ, the parameters η_1 and η_2 must satisfy the inequality:

$$
1 + 2\eta_2 \sin^2 \varphi + (\eta_1 - 2\eta_2) \sin^4 \varphi > 0.
\tag{2.4}
$$

This condition is reduced to

$$
\eta_2 \geq 0 \quad \text{or} \quad \eta_1 - 2\eta_2 - \eta_2^2 \geq 0.
\tag{2.5}
$$

We will assume this condition below. Then we obtain the following results: If

$\eta_2 \leq 0$,

$$\max_{k,\varphi} \lambda(k, \varphi) = \lambda(k_c, \varphi_c)$$

$$= R - 1 + \frac{\eta_1 - 2\eta_2}{\eta_1 - 2\eta_2 - \eta_2^2}, \tag{2.6}$$

where

$$k_c = \sqrt{\frac{\eta_1 - 2\eta_2 - \eta_2^2}{\eta_1 - 2\eta_2}} \quad \text{and} \quad \sin^2 \varphi_c = -\frac{\eta_2}{\eta_1 - 2\eta_2}. \tag{2.7}$$

The critical control parameter R_c is then expressed as

$$R_c = -\frac{\eta_2^2}{\eta_1 - 2\eta_2 - \eta_2^2}. \tag{2.8}$$

On the other hand, if $\eta_2 \geq 0$,

$$\max_{k,\varphi} \lambda(k, \varphi) = \lambda(k_c, \varphi_c)$$

$$= R, \tag{2.9}$$

where

$$k_c = 1 \quad \text{and} \quad \sin^2 \varphi_c = 0. \tag{2.10}$$

In this case, the critical control parameter R_c is determined as

$$R_c = 0. \tag{2.11}$$

These results show that $\eta_2 = 0$ corresponds to the Lifshitz point: $\eta_2 < 0$ holds for the oblique roll regime, whereas $\eta_2 > 0$ holds for the normal roll regime[39]. We may thus interpret η_2 as the distance from the Lifshitz point. Since we are concerned with the normal roll regime, $\eta_2 > 0$ will be assumed below.

The Pesch-Kramer model also has a potential. Therefore, the dynamics is relaxational tending to the roll solution which minimizes the potential, and its time scale is much shorter than that for an isotropic system due to the uniqueness

of the potential minimum. Since we found that their model equation is too simple to describe defect chaos, we consider a more complex model; a model supplmented with drift terms, which is written as

$$\dot{w} + (\vec{U} \cdot \vec{\nabla})w = Rw - w^3 + \hat{D}w, \qquad (2.12a)$$

$$\hat{D} = -(1+\triangle)^2 - \eta_1 \partial_y{}^4 - 2\eta_2 \partial_x{}^2 \partial_y{}^2.$$

The drift field $\vec{U}$ is induced by the deformation of the rolls. The equation for $\vec{U}$ can be determined by the following requirements[59]. The first is that the drift field $\vec{U}$ determined adiabatically by the vertical velocity w. Second, it must be invariant under the transformations : (1) $x \to -x, U_x \to -U_x$, (2) $y \to -y, U_y \to -U_y$ and (3) $w \to -w$. The third requirement is that the equation should include spatial derivatives at most up to the third order and the powers of w up to the second order. Finally, the drift field should satisfy the incompressibility condition. From these requirements, the equation can be written in the form

$$U_i = \partial_i[a_i w^2 + \sum_j \{b_{ij} w \partial_j^2 w + c_{ij}(\partial_j w)^2\}]$$

$$+ \sum_j h_{ij} w \partial_i \partial_j^2 w - \partial_i p, \qquad (2.12b)$$

$$\vec{\nabla} \cdot \vec{U} = 0. \qquad (2.12c)$$

Here, the suffixes $i, j \cdots$ represent x or y, and we introduced an auxiliary field p which represents effective pressure. Although many parameters appear in eq.(2.12), they are not actually indepedent because eq.(2.12) is invariant under the transformations: $(1)a_1 \to a_1 + v_1$, $b_1 \to b_1 + v_1$ $(2)a_{2j} \to a_{2j} + v_{2j}$, $b_{2j} \to b_{2j} + v_{2j}$, $(3)a_{3j} \to a_{3j} + v_{3j}$, $b_{3j} \to b_{3j} + v_{3j}$, where v_1, v_{2j} and v_{3j} are arbitrary constants. Therefore, we can set $a_y = b_{yj} = c_{yj} = 0$ without loss of generality, and if the drift satisfies the rotational symmetry, we can further set $a_x = b_{xj} = c_{xj} = 0$ and $h_{ij} = h$.

We now further simplify the model so that the analysis may become easier. We treat w as a complex field W. One may then interpret $Re(W)$ as the vertical velocity. We also assume $a_x = b_{xj} = c_{xj} = 0$. Then the model equation becomes

$$\dot{W} + (\vec{U} \cdot \vec{\nabla})W = RW - |W|^2 W + \hat{D}W, \tag{2.13a}$$

$$\hat{D} = -(1 + \Delta)^2 - \eta_1 \partial_y{}^4 - 2\eta_2 \partial_x{}^2 \partial_y{}^2.$$

$$U_i = \sum_j h_{ij}(W^* \partial_i \partial_j^2 W + c.c) - \partial_i p, \tag{2.13b}$$

$$\vec{\nabla} \cdot \vec{U} = 0. \tag{2.13c}$$

We will call this model Model(A). If the drift is approximated as isotropic, then we obtain an even simpler model equation:

$$\dot{W} + (\vec{U} \cdot \vec{\nabla})W = RW - |W|^2 W + \hat{D}W, \tag{2.14a}$$

$$\hat{D} = -(1 + \Delta)^2 - \eta_1 \partial_y{}^4 - 2\eta_2 \partial_x{}^2 \partial_y{}^2.$$

$$U_i = h(W^* \partial_i \Delta W + c.c) - \partial_i p, \tag{2.14b}$$

$$\vec{\nabla} \cdot \vec{U} = 0. \tag{2.14c}$$

We will call this model Model(B).

We can also express the drift terms in different forms such as an integral representation and a vorticity representation. Let us consider these expressions for Model(B) only. (Similar arguments can apply to Model(A).) We first explain the integral representation. The pressure field p is determined by the Poisson equation derived from eqs.(2.14b) and (2.14c):

$$\Delta p = h \sum_i \partial_i (W^* \partial_i \Delta W + c.c). \tag{2.15}$$

This equation shows that the pressure field is determined nonlocally. Substituting eq.(2.15) into eq.(2.14b), we can obtain an integral representations for the drift

field:

$$U_i = \sum_j \int d^2 x' P_{ij}(\vec{x} - \vec{x}')h(W^* \partial_j \triangle W(\vec{x}') + c.c), \qquad (2.16)$$

where P_{ij} is defined as

$$P_{ij}(\vec{x}) = \delta_{ij}(\vec{x}) - \partial_i \partial_j G(\vec{x}),$$
$$\triangle G(\vec{x}) = \delta(\vec{x}). \qquad (2.17)$$

We next explain the vorticity representation. From eq.(2.14c), we can express the drift field $\vec{U}$ in terms of a stream function ψ as

$$\vec{U} = (\partial_y \psi, -\partial_x \psi), \qquad (2.18)$$

and ψ is related to the vertical vorticity ζ through $\zeta = -\triangle \psi$. Then, from eq.(2.14b), we obtain the vorticity equation:

$$-\triangle \psi = h\hat{z}(\vec{\nabla} W^* \times \vec{\nabla} \triangle W + c.c) \qquad (2.19)$$

This expression is a standard form for the drift terms[55-58].

We can easily find that the drift terms do not contribute to the amplitude equation in the lowest order calculation. Therefore, our models have stable roll solutions at least near the onset of convections. The behavior at a finite distance apart from the onset of convection must still be considered. We will investigate it in a few sections below.

3. Phase Dynamics

The phase dynamics in convection problems was first presented by Pomeau and Manneville[46], and they derived a linear phase diffusion equation. In the Pomeau-Manneville theory, a reference state or the background wavevector is introduced, which means that there is one phase dynamics for each reference state. Since the dynamics should be independent of the reference state, the phase equation must be free from the reference state chosen or invariant under an arbitrary change of the reference state. Obviously, the linear phase equation can not satisfy this requirement. A non-linear theory must therefore be developed. As one possible approach, a simple extension including higher order terms may be considered. In that case, the phase equation can be invariant under an infinitely small change of the reference state. If we require the invariance under a finite change of the reference state, however, we need the infinite order terms. In order to avoid this difficulty, Cross and Newell presented an more efficient approach, in which the phase is defined to be independent of the reference state[44,60,61].

In this section, we consider the phase dynamics for Model(A) following the Cross-Newell theory. This equation has a family of stationary periodic solutions and these are analytically expressed as

$$
\begin{aligned}
W_s &= A(\vec{k})e^{i\theta}, \\
\theta &= \vec{k} \cdot \vec{x} + \varphi, \\
A(\vec{k}) &= (R - (k^2 - 1)^2 - \eta_1 k_y^4 - 2\eta_2 k_x^2 k_y^2)^{\frac{1}{2}},
\end{aligned}
\tag{3.1}
$$

where $k^2 = k_x^2 + k_y^2$, $\vec{k} = (k_x, k_y)$ is the wavevector of the rolls and φ is an arbitrary constant.

We now investigate the local stability of the roll solutions, i.e. the stability for the local disturbance. The *local* disturbance means the disturbance for a pair of rolls which is extended periodically when the rolls are infinitly aligned. Thus, the space of the *local* disturbance is defined as

$$
V = \{u \mid u = u_1 + iu_2; u_1, u_2 \in L^2(0, 2\pi); u(\theta) = u(\theta + 2\pi)\}
$$

and the inner product (f, g) for $f, g \in V$ as

$$(f, g) = \int_0^{2\pi} d\theta (f_1 g_1 + f_2 g_2) = Re \int_0^{2\pi} d\theta f^* \cdot g, \qquad (3.2)$$

where $f_1 = Re(f)$, $f_2 = Im(f)$, $g_1 = Re(g)$ and $g_2 = Im(g)$. The local stability of the solution W_s is determined by the linear equation for the local disturbance u:

$$\dot{u} = \hat{L}_0 \cdot u, \qquad (3.3)$$

where the operator $\hat{L}_0$ is defined as

$$\hat{L}_0 \cdot u = Ru + \hat{D}_0 u - 2|W_s|^2 u - W_s^2 u^*, \qquad (3.4)$$
$$\hat{D}_0 = -(1 + k^2 \partial_\theta)^2 - \eta_1 k_y^4 \partial_\theta^4 - 2\eta_2 k_x^2 k_y^2 \partial_\theta^4.$$

The operator $\hat{L}_0$ is semi-negative definite and has a zero eigenvalue. Then the corresponding neutral mode Φ_0 satisfies

$$\hat{L}_0 \cdot \Phi_0 = 0, \qquad (3.5)$$

and its adjoint vector $\Phi_0^\dagger$ is identical with the original neutral mode due to the Hermiticity of $\hat{L}_0$:

$$\Phi_0^\dagger = \Phi_0. \qquad (3.6)$$

We can easily check $\Phi_0 = \partial_\theta W_s$. This implies that the roll solutions are neutrally stable against the disturbance corresponding to a space translation and stable against the other *local* disturbances. Note that the existence of the neutral mode stems from the translational symmetry. Borrowing a field-theoretical term[62], we may thus call the neutral mode the Goldstone mode.

Since the local stability of the roll solutions is guaranteed, we now investigate large scale behavior. We first notice that there are two characteristic scales of length in the system: one is the wavelength of periodic patterns and the other

is the system size. Since we are concerned with the system of large aspect ratio μ^{-1}, it is appropriate to introduce a scaled coordinate system $(\theta, \vec{X}, T)$, where θ is a periodic coordinate representing the local structure, and $(\vec{X}, T)$ are the large scale coordinates such that $\vec{X} = \mu\vec{x}$, $T = \mu t$ and $\mu \ll 1$. Then a field f on space $(\theta, \vec{X})$ is expressed by

$$f = f(\theta, \vec{X}) = \sum_j f_j(\vec{X})\Phi_j(\theta), \tag{3.7}$$

where Φ_j is an eigenvector of $\hat{L}_0$ and $\{\Phi_j\}$ forms a complete set of basis in V. Further, the space derivatives are substituted as

$$\partial_i = k_i\partial_\theta + \mu\partial_j',$$
$$\partial_j' = \frac{\partial}{\partial X_j}. \tag{3.8}$$

Let us consider the dynamics of the disturbance $\rho(\theta, \vec{X})$ around a stationary solution W_s. Since the components $\rho_j(\vec{X})$ $(j \neq 0)$ decay rapidly, the relevant dynamical variable in the long term behavior is only $\rho_0(\vec{X})$. This is nothing but a phase variable which represents the large scale variation of the wavevector $\vec{k}$. However, it is not very easy to derive directly dynamics of ρ_0. Thus, the local wavevector $\vec{k}(\vec{X}, T)$ and the phase $\Theta(\vec{X}, T)$ such as $k_i = \partial_i'\Theta$ are introduced and the dynamics of phase Θ will be derived. We express the deformation of the rolls as

$$W = A(\vec{k}(\vec{X}, T))e^{i\theta} + \rho(\theta, \vec{X}, T), \tag{3.9}$$

where ρ is the part of deformation which can not be absorbed into the local wavevector $\vec{k}(\vec{X}, T)$, and satisfies

$$(\Phi_0^\dagger, \rho) = \rho_0(\vec{X}, T) = 0. \tag{3.10}$$

Since ρ is perturbatively determined, we expand it in the form:

$$\rho = \mu\rho^{(1)} + \mu^2\rho^{(2)} + \cdots. \tag{3.11}$$

We substitute eqs.(3.8),(3.9) and (3.11) into the model equation and arrange the

terms according to various powers in μ. In this way, we obtain the equation at order μ:

$$(\dot{\Theta} + \vec{U}^{(1)} \cdot \hat{k})\partial_\theta W = \hat{D}_1 W + \hat{L}_0 \rho^{(1)}, \qquad (3.12a)$$

$$U_i^{(1)} = -\sum_{l,m} \beta_{ilm} \partial_l' \partial_m' \Theta - \partial_i p, \qquad (3.12b)$$

$$\vec{\nabla} \cdot \vec{U}^{(1)} = 0, \qquad (3.12c)$$

where $\vec{U} = \mu \vec{U}^{(1)} + \cdots$ and $\hat{D} = \hat{D}_0 + \mu \hat{D}_1 + \cdots$. Finally, the inner product of $\Phi_0^\dagger$ with this equation yields the phase equation of the form:

$$\dot{\Theta} + \vec{U} \cdot \hat{k} = \sum_{ij} \alpha_{ij}(\vec{k}) \partial_i \partial_j \Theta, \qquad (3.13a)$$

$$U_i = -\sum_{l,m} \beta_{ilm}(\vec{k}) \partial_l \partial_m \Theta - \partial_i p, \qquad (3.13b)$$

$$\vec{\nabla} \cdot \vec{U} = 0, \qquad (3.13c)$$

where we dropped unnecessary shoulder notions, and the expressions for the tensors α_{ij} and β_{ilm} are calculated to give

$$\alpha_{ij}(\vec{k}) = 2(k^2 - 1)\delta_{ij} + 4(k^2 - 1)k_i k_j \frac{\partial A^2}{\partial k_j^2}\frac{1}{A^2} + 4k_i k_j + \eta_1 \alpha_{ij}^{(A1)} + \eta_2 \alpha_{ij}^{(A2)},$$

$$\alpha_{ij}^{(A1)} = 6k_y^2 \delta_{iy}\delta_{jy} + 4k_i^3 k_j \frac{\partial A^2}{\partial k_j^2}\frac{1}{A^2}\delta_{iy},$$

$$\alpha_{ij}^{(A2)} = (2k_y^2 + 4k_x^2 k_y^2 \frac{\partial A^2}{\partial k_x^2}\frac{1}{A^2})\delta_{ix}\delta_{jx} + (2k_x^2 + 4k_x^2 k_y^2 \frac{\partial A^2}{\partial k_y^2}\frac{1}{A^2})\delta_{iy}\delta_{jy}$$

$$+ (8k_x k_y + 4k_x^3 k_y \frac{\partial A^2}{\partial k_x^2}\frac{1}{A^2} + 4k_y^3 k_x \frac{\partial A^2}{\partial k_y^2}\frac{1}{A^2})\delta_{iy}\delta_{jx},$$

$$\beta_{ilm}(\vec{k}) = 2h_{im}k_i A^2 (\delta_{ml} + 2k_m k_l \frac{\partial A^2}{\partial k_l^2}\frac{1}{A^2})$$

$$+ 2\sum_j h_{ij} A^2 \delta_{im} k_l (2\delta_{jl} + k_j^2 \frac{\partial A^2}{\partial k_l^2}\frac{1}{A^2}).$$

$$(3.14)$$

We note that eq.(3.13) has nonlocal property which is inherited from the

original model equation. Let us clarify the nonlocal nature by eliminating the supplemental field p from eq.(3.13). After elimination, we obtain an integral representation of the phase equation :

$$\dot{\Theta} + \vec{U} \cdot \vec{k} = \sum_{ij} \alpha_{ij}(\vec{k}) \partial_i \partial_j \Theta,$$

$$U_i = - \sum_{jlm} \int d^2 x' P_{ij}(\vec{x} - \vec{x}') \cdot \beta_{jlm}(\vec{k}') \partial_l \partial_m \Theta(\vec{x}'),$$

$$(3.15)$$

where $\vec{k}' = \vec{k}(\vec{x}')$, and the projection operator P_{ij} was defined by eq.(2.17). We can further eliminate the drift field $\vec{U}$ and rewrite the phase equation only in terms of the phase field :

$$\dot{\Theta} = \sum_{ij} \int d^2 x' Q_{ij}(\vec{x}, \vec{x}') \partial_i \partial_j \Theta(\vec{x}'),$$

$$Q_{ij}(\vec{x}, \vec{x}') = \alpha_{ij}(\vec{k}) \delta(\vec{x} - \vec{x}') + \sum_{lm} k_l(\vec{x}) P_{lm}(\vec{x} - \vec{x}') \beta_{mij}(\vec{k}').$$

$$(3.16)$$

The above equation makes contrast with the phase equation in the case of free boundary conditions. (see section 7.)

Recalling $k_i = \partial_i \Theta$, we note further that eq.(3.16) is non-linear. Although it is difficult to solve this equation in general, it provides some useful informations. As a few examples, the linear stability analysis and the weakly nonlinear analysis near the phase instability are easily carried out on the basis of this equation. These will be shown in the next two sections.

4. Linear Stability Analysis of Normal Rolls

Linear stability of a normal roll solution W_s is generally determined by the linear equation:

$$\dot{u} = \hat{L} \cdot u, \qquad (4.1)$$

which is obtained by substituting $W = W_s + u$ into the model equation and linearizing it in u. The dynamics of this equation is under the control of the eigenvalues of the operator $\hat{L}$, although long calculations would be needed to derive all eigenvalues of $\hat{L}$. Since we are especially interested in the phase instability or the modulational instability, we focus on the long-wavelength modes and work with the phase equation[36,46].

The normal roll solutions of the phase equation eq.(3.16) are expressed by $\Theta = k_0 x$ up to an arbitrary phase constant. Let us now argue the stability of this solution. Substituting $\Theta = k_0 x + \phi$ into eq.(3.16) and linearizing it in ϕ, we obtain a linear phase equation :

$$\dot{\phi} = \sum_{ij} \alpha_{ij}^0 \partial_i \partial_j \phi + k_0 \sum_{ilm} \beta_{jlm}^0 \int d^2 x' P_{xj}(\vec{x} - \vec{x}') \partial_l \partial_m \phi(\vec{x}'), \qquad (4.2)$$

where $\alpha_{ij}^0 = \alpha_{ij}(\vec{k}_0)$, $\beta_{ilm}^0 = \beta_{ilm}(\vec{k}_0)$ and $\vec{k}_0 = (k_0, 0)$. From this equation, the growth rate $\lambda(\vec{q})$ for the phase disturbance with wavevector $\vec{q}$ is derived as

$$\begin{aligned}
\lambda(\vec{q}) &= -\sum_{ij} \alpha_{ij}^0 q_i q_j - k_0 \sum_{jlm} (\delta_{xj} - \frac{q_x q_j}{q^2}) \beta_{jlm}^0 q_l q_m \\
&= -\alpha_{xx}^0 q_x^2 - \alpha_{yy}^0 q_y^2 - k_0 \frac{q_y^2}{q^2} (\tilde{\beta}_{xxx}^0 q_x^2 + \beta_{xyy}^0 q_y^2),
\end{aligned} \qquad (4.3)$$

where $\tilde{\beta}_{xxx}^0 = \beta_{xxx}^0 - \beta_{yxy}^0$, and the expressions for α_{ij}^0 and β_{ilm}^0 are listed up as

$-20-$

follows:

$$\alpha_{xx}^0 = 2(3k_0^2 - 1) - \frac{8(k_0^2 - 1)^2 k_0^2}{A^2}, \qquad \alpha_{yy}^0 = 2(k_0^2 - 1) + 2k_0^2 \eta_2,$$

$$\alpha_{xy}^0 = \alpha_{yx}^0 = 0,$$

$$\beta_{xxx}^0 = 6h_{xx}k\{A^2 - 2k_0^2(k_0^2 - 1)\}, \qquad \beta_{yxy}^0 = 4h_{yx}k\{A^2 - k_0^2(k_0^2 - 1)\}, \qquad (4.4)$$

$$\beta_{xyy}^0 = 2h_{xy}k_0 A^2,$$

$$\beta_{xxy}^0 = \beta_{yxx}^0 = \beta_{yyy}^0 = \beta_{yxy}^0 = 0.$$

Note that the growth rate $\lambda(\vec{q})$ is nothing but the long-wavelength part of the eigenvalues of $\hat{L}$, and therefore short-wavelength instability such as cross roll instability or oblique roll instability can not be investigated by the analysis based on the phase equation.

Let us classify the types of the phase instability by specifying the most unstable directions[48,49]. Setting $q_x = q \cos \vartheta$ and $q_y = q \sin \vartheta$, we rewrite eq.(4.3) as

$$\lambda(\vec{q}) = -d(\vartheta)q^2,$$

$$d(\vartheta) = \alpha_{xx}^0 \cos^2 \vartheta + \alpha_{yy}^0 \sin^2 \vartheta + k_0 \sin^2 \vartheta(\tilde{\beta}_{xxx}^0 \cos^2 \vartheta + \beta_{xyy}^0 \sin^2 \vartheta), \qquad (4.5)$$

$$= a \sin^4 \vartheta + b \sin^2 \vartheta + c,$$

where a, b and c were set as

$$a = k_0(\beta_{xyy}^0 - \tilde{\beta}_{xxx}^0),$$

$$b = k_0 \tilde{\beta}_{xxx}^0 + \alpha_{yy}^0 - \alpha_{xx}^0, \qquad (4.6)$$

$$c = \alpha_{xx}^0,$$

Here we may interpret $d(\vartheta)$ as a diffusion constant in the direction making angle ϑ from the x-direction. The growth rate $\lambda(\vec{q})$ is not regular at $\vec{q} = \vec{0}$ as shown by eq.(4.3). Therefore, we can not expand $\lambda(\vec{q})$ like $\lambda(\vec{q}) = \sum_{ij} D_{ij} q_i q_j + \cdots$. This implies that the diffusion constants in these systems are not well-defined. However, when we consider the disturbance with one direction, the diffusion

constant in this direction becomes well-defined as expressed by eq.(4.5). We can thus define the most dangerous direction ϑ_* and the diffusion constant in this direction as

$$\vartheta_* = \arg\min_{\vartheta} d(\vartheta),$$
$$d_* = d(\vartheta_*),$$

(4.7)

Then the phase instability occurs when the phase diffusion constant becomes negative, i.e. $d_* < 0$, and the type of the phase instability is called

$$\begin{cases} \text{the Eckhaus instability,} & \text{if } \vartheta_* = 0; \\ \text{zigzag instability,} & \text{if } \vartheta_* = \pi/2; \\ \text{skewed varicose instability,} & \text{otherwise.} \end{cases}$$

We notice that if the drift terms are absent, the skewed varicose instability never occurs because $a = 0$.

We now investigate the conditions for the phase instability. Let us restrict ourselves to the rolls with the wavevector $\vec{k}_0 = (1, 0)$ at the onset of convections. In that case, a, b and c in eq.(4.6) are calculated from eq.(4.4) as

$$a = 2R(h - h'), \quad b = 2Rh' + 2\eta_2 - 4, \quad c = 4,$$

(4.8)

where $h = h_{xy}$ and $h' = 3h_{xx} - 2h_{yx}$. These expressions give us the following results:

[1] The Eckhaus instability does not occur,

[2] The zigzag instability occurs when $R > -\eta_2/h$ under the condition

$$h < 0 \quad \text{and} \quad h' \geq \min(h, \frac{2 - \eta_2}{R}, 2h - \frac{2 - \eta_2}{R}),$$

(4.9)

[3] The skewed varicose instability occurs when

$$h'^2 R^2 - 2(4h - 4h' + 2 - \eta_2)R + (2 - \eta_2)^2 > 0,$$

(4.10)

under the condition

$$h' < \min(h, \frac{2 - \eta_2}{R}, 2h - \frac{2 - \eta_2}{R}).$$

(4.11)

Then, either eqs.(4.9) or (4.11) should hold in order that normal rolls may

become unstable at $R'_c > R_c = 0$. If we consider Model(B) in which the isotropy of the drift field was assumed,i.e. $h_{ij} = h' = h$, the relevant instability is only the zigzag instability because eq.(4.11) do not hold, and the zigzag instability occurs beyond $R'_c = -\eta_2/h$ when the condition $h < 0$ is satisfied. A recent experiment by Nasuno and Kai[31] seems to support the fact that the normal rolls become unstable through the zigzag instability except that the type of instability of normal rolls turns into the skewed varicose instability at $R''_c > R'_c$. We must thus consider Model(A) so that we may explain this experimental fact. We obtain the results: the necessary and sufficient condition for the occurence of the change of the instability type is that the inequalities

$$h' < 2h < 0 \qquad \text{and} \qquad 0 < \eta_2 < 2, \tag{4.12}$$

are satisfied. In this case R''_c is calculated as

$$R''_c = \frac{2 - \eta_2}{2h - h'}. \tag{4.13}$$

So far, we focused on the local behavior in the phase space, i.e. the behavior near the most important stationary solution. We now look into global structures in the phase space so that we may understand completely the system behavior. In particular, we investigate the stability of all normal roll solutions, and consider the stability diagram in the space (R, k_x). This corresponds to the Busse balloon in the case of the Rayleigh-Bénard convection[49]. We show two examples from several types of stability diagrams. The first is the stability diagram for Model(B) under the condition $h < 0$, which is shown in fig.1(a). The analytic expressions of the marginal stability lines are derived from $\alpha_{xx}^0 = 0$ and $\alpha_{yy}^0 + k_0\beta_{xyy}^0 = 0$ so that R may satisfy $R = R_z(k)$ for the zigzag instability and $R = R_E(k)$ for the Eckhaus instability, where

$$
\begin{aligned}
R_z(k) &= (k^2 - 1)^2 - \frac{k^2 - 1}{hk^2} - \frac{\eta_2}{h}, \\
R_E(k) &= \frac{(k^2 - 1)^2(7k^2 - 1)}{(3k^2 - 1)}.
\end{aligned}
\tag{4.14}
$$

Second, we show the stability diagram for the case that the change of the instability type occurs. (see fig.1(b).) The analytic expressions of the marginal stability lines are the same as the first example, and the line on which the type of instability changes from the zigzag instability into the skewed varicose instability is expressed as

$$R = R_s(k) = (k^2 - 1)^2 + \frac{p + \sqrt{p^2 + 16(2h - h')(k^2 - 1)^2}}{2h - h'}, \qquad (4.15)$$
$$p = 2 - \eta_2 - 4(k^2 - 1)h'',$$

where a parameter $h'' = (3h_{xx} - h_{yx})/2$ was introduced. These stability diagrams are quite similar to the one obtained by Nasuno and Kai (see fig.1(c).), and show that stable domains are bounded in the space (k_x, R). Therefore, the solution with a *natural* wavenumber, which may be different from the wavenumber at the onset, becomes unstable. The system behavior should then be determined by the nonlinear property. In the next section, we consider the weakly nonlinear analysis near the phase instability.

Note that there are other types of stability diagrams in general, of which the transition through the skewed varicose instability would be of great interest. In the present paper, we will not treat this case, but concentrate on the transition through the zigzag instability.
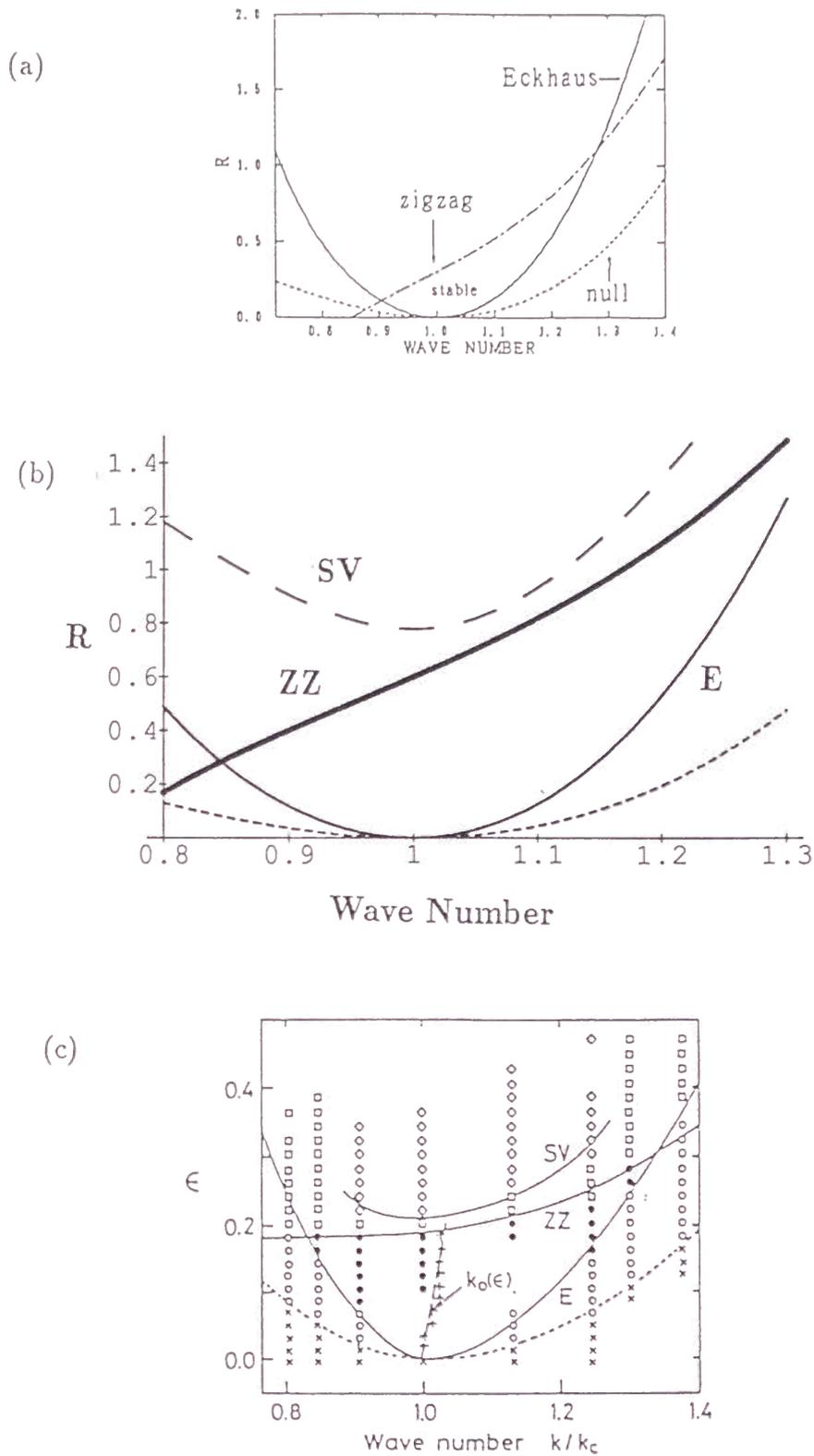
(a)

(b)

(c)

Fig.1 Stability Diagrams for (a) Model(B) ($\eta_2 = 0.3$, $h = -1.0$),(b)Model(A) ($\eta_2 = 0.6$, $h = -1.0$, $h' = -3.8$ $h'' = 0$), and (c) experimental results by Nasuno and Kai.

5. Weakly Nonlinear Analysis

In weakly nonlinear analysis, non-linear terms are perturbatively taken into account. In the present case, the distance ε from the onset of the phase instability is regarded as a small parameter. Since the phase instability is related to a negative diffusion constant in the phase equation, the phase dynamics approach can be considered as a weakly nonlinear analysis. This idea was first presented by Kuramoto[45,47]. Following Kuramoto we will derive the phase equation near the zigzag instability. We first notice the scaling form of phase ϕ when $\varepsilon \to 0$. Since the Fourier basis are the eigenvectors of the linear operator $\hat{L}$, the corresponding eigenvalues σ are characterized by the wavevector $\vec{q}$ like $\sigma = \sigma(q_x, q_y)$. Then, for $\varepsilon = -\alpha_{yy}^0 - k_0\beta_{xyy}^0 \to 0$, the scaling relation holds in the form

$$\sigma(q_x, q_y) = \varepsilon^2 \bar{\sigma}(\varepsilon q_x, \varepsilon^{1/2} q_y). \tag{5.1}$$

This implies that the phase satisfies the following scaling form for $\varepsilon \to 0$:

$$\phi(x, y, t) = \bar{\phi}(\varepsilon x, \varepsilon^{1/2} y, \varepsilon^2 t). \tag{5.2}$$

Let us now look into some symmetry properties of the phase equation. The phase equation must be invariant under the transformations: $(1) x \to -x, \phi \to -\phi$, $(2) y \to -y$ and $(3) \phi \to \phi + \phi_0$, where ϕ_0 is an arbitrary constant. From these requirements, the phase equation near the zigzag instability can be written as

$$\begin{aligned}
\dot{\phi} = &-\varepsilon\partial_y{}^2\phi - D_4\partial_y{}^4\phi + D\partial_x{}^2\phi + g(\partial_y\phi)^2\partial_y{}^2\phi \\
&+ s_1(\partial_x\phi)\partial_y{}^2\phi + s_2(\partial_y\phi)\partial_x\partial_y\phi,
\end{aligned} \tag{5.3}$$

although the last term was overlooked in Kuramoto's paper[47,63]. The coefficients of this equation can be calculated from the phase equation eq.(3.16).

$-26-$

Substituting $\Theta = k_0 x + \phi$ into α_{ij} and β_{ilm}, we obtain the expansions:

$$\alpha_{ij} = \alpha_{ij}^0 + \left(\frac{\partial \alpha_{ij}}{\partial k_x}\right)^0 \partial_x \phi + \left(\frac{\partial \alpha_{ij}}{\partial k_y}\right)^0 \partial_y \phi + \left(\frac{\partial \alpha_{ij}}{\partial k_y^2}\right)^0 (\partial_y \phi)^2 \cdots,$$

$$\beta_{ilm} = \beta_{ilm}^0 + \left(\frac{\partial \beta_{ilm}}{\partial k_x}\right)^0 \partial_x \phi + \left(\frac{\partial \beta_{ilm}}{\partial k_y}\right)^0 \partial_y \phi + \left(\frac{\partial \beta_{ilm}}{\partial k_y^2}\right)^0 (\partial_y \phi)^2 \cdots.$$

(5.4)

We expand formally $\hat{P}_{ij}$ as

$$\hat{P}_{xx} = 1 - \frac{\partial_x^2}{\partial_x^2 + \partial_y^2} = 1 - \hat{M}^2 + \hat{M}^4 + \cdots,$$

$$\hat{P}_{xy} = -\frac{\partial_x \partial_y}{\partial_x^2 + \partial_y^2} = -\hat{M} + \hat{M}^3 + \cdots,$$

(5.5)

$$\hat{P}_{yy} = 1 - \frac{\partial_y^2}{\partial_x^2 + \partial_y^2} = \hat{M}^2 - \hat{M}^4 + \cdots,$$

where we introduced an operator $\hat{M} = \partial_x/\partial_y \sim \varepsilon^{1/2}$. Substituting $\Theta = k_0 x + \phi$, eqs.(5.4) and (5.5) into eq.(3.16), we obtain the coefficients of the phase equation eq.(3.3) in the form:

$$D = \alpha_{xx}^0 + k_0(\tilde{\beta}_{xxx}^0 - \beta_{xyy}^0),$$

$$g = \left(\frac{\partial \alpha_{yy}}{\partial k_y^2}\right)^0 + k_0\left(\frac{\partial \beta_{xyy}}{\partial k_y^2}\right)^0,$$

$$s_1 = \left(\frac{\partial \alpha_{yy}}{\partial k_x}\right)^0 + k_0\left(\frac{\partial \beta_{xyy}}{\partial k_x}\right)^0 + \beta_{xyy}^0,$$

$$s_2 = \left(\frac{\partial \alpha_{xy}}{\partial k_y}\right)^0 + \left(\frac{\partial \alpha_{yx}}{\partial k_y}\right)^0 - \beta_{xyy}^0 + \beta_{yxy}^0,$$

(5.6)

Note that the phase equation is nonlocal in general. However, if we restrict ourselves to the neighborhood of the zigzag instability, nonlocality becomes negligible in the lowest order expansions in ε. Furthermore, when we focus on the roll solution with the onset wavevector, we may put $k_0 = 1$ in eq.(5.6). The

$-27-$

coefficients in eq(5.6) are then expressed as

$$
\begin{aligned}
D &= 4, \\
g &= 6(1 + \eta_1) - 4h\eta_2 > 0, \\
s_1 &= 4(1 + \eta_2), \\
s_2 &= 2(4 + 3\eta_2).
\end{aligned}
\tag{5.7}
$$

We now investigate the behavior of the solution of eq.(5.3) in further detail. When ε is positive, the solution $\phi = const.$ becomes unstable and the disturbance in the y direction grows. As a result, the x-dependence of ϕ may be neglected at first, and we obtain the equation:

$$
\dot{\phi} = -\varepsilon\partial_y{}^2\phi - D_4\partial_y{}^4\phi + g(\partial_y\phi)^2\partial_y{}^2\phi.
\tag{5.8}
$$

This equation is also expressed as

$$
\dot{u} = -\partial_y{}^2(\varepsilon u - \frac{1}{3}gu^3 + D_4\partial_y{}^2 u),
\tag{5.9}
$$

where $u = \partial_y\phi$. Equation(5.9) is identical to the Ginzburg-Landau equation for a conserved order parameter u as it arises in spinodal decomposition[64]. A similar phase equation was discussed by Brand and Deissler in the problem of confined states[65,66], and also by Riecke in parametrically excited standing wave[67].

Since the sign of the coefficient g is positive, the bifurcation is supercritical, and $u = \pm\sqrt{3\varepsilon/g}$ which minimizes the potential gives the stable states. Though the uniform states $u = \pm\sqrt{3\varepsilon/g}$ will not be realized in general due to its violation of the conservation law, the boundedness of the phase deformation will be ensured at least. What is expected to occur is the formation of kink-antikink pairs and their dynamics with very long time scale[68]. Note that kink-antikink patterns in u implies zigzag patterns in convective rolls.

We next consider the effect of the variation in the x-direction and investigate the stability of the uniform states $u = \pm\sqrt{3\varepsilon/g}$. Then we obtain the following

results: If $g > g_c$, the zigzag roll remains stable because the uniform states $u = \pm\sqrt{3\varepsilon/g}$ are stable. On the contrary, if $0 < g < g_c = 3s_2^2/8D$, the uniform states $u = \pm\sqrt{3\varepsilon/g}$ become unstable against the disturbance with direction slightly different from the y-direction. The dynamics is essentially two dimensional as for the dynamics associated with the skewed varicose instability in the Rayleigh-Bénard convection. It would be necessary to investigate in further detail such two-dimensional dynamics for a full understanding of the system behavior.

In our model, the value g_c is calculated from eq.(5.7), and it turn out to be

$$g_c = \frac{3(4 + 3\eta_2)^2}{8}. \tag{5.10}$$

This expression shows that $g > g_c$ holds for sufficiently small η_2 and that $0 < g < g_c$ holds for sufficiently large η_2. This implies that the stable zigzag roll appears sufficiently close to the Lifshitz point, while defect creation through the instability of the zigzag roll occurs far from the Lifshitz point. These results are consistent with experiments, and therefore there is a possibility that defect chaos occurs in the case $0 < g < g_c$. This will be checked by numerical simulations in the next section.

6. Numerical Simulations

In this section, the behavior of Model(B) will be investigated numerically. When a PDE is defined in a finite domain D, we must impose boundary conditions. The most realistic ones are [55]

$$W|_{\partial D} = (\vec{n} \cdot \vec{\nabla})W|_{\partial D} = \psi|_{\partial D} = 0, \tag{6.1}$$

where $\vec{n}$ is the unit vector normal to the boundary. Since it is difficult to simulate the PDE model directly, we follow Oono and Puri[51,52] and take a CML model corresponding to the vorticity representation of Model(B). Oono and Puri presented the essential idea that the local and global processes can be separated. Let us define a cell dynamics of a complex variable $W(i,j)$ on each cell in the the square lattice of the size $N \times N$:

$$\widetilde{W}_{n+1} = \frac{\sqrt{R}W_n}{\left(Re^{-2R\Delta t} + |W_n|^2(1 - e^{-2R\Delta t})\right)^{\frac{1}{2}}}, \tag{6.2a}$$

where Δt is the time increment in each step. This map was obtained through the integration of the ordinary differential equation:

$$\dot{W} = RW - |W|^2 W.$$

We next connect the maps on different cells in the following manner:

$$W_{n+1} = \widetilde{W}_{n+1} - (\vec{U}_{n+1} \cdot \vec{\nabla})\widetilde{W}_{n+1} + \hat{D}\widetilde{W}_{n+1}, \tag{6.2b}$$

$$\hat{D} = -(\Delta t)\{(1 + \Delta)^2 + \eta_1 \partial_y{}^4 + 2\eta_2 \partial_x{}^2 \partial_y{}^2\},$$

$$\vec{U}_{n+1} = (\partial_y \psi_{n+1}, -\partial_x \psi_{n+1}), \tag{6.2c}$$

$$-\triangle \psi_{n+1} = (\Delta t)h\hat{z}(\vec{\nabla}\widetilde{W}_{n+1}^* \times \vec{\nabla}\triangle\widetilde{W}_{n+1} + c.c.). \tag{6.2d}$$

Here, we used derivative notations although we replaced the spatial derivative by the cell-to-cell difference with the space increment Δx. We also introduced a real

variable $\psi(i,j)$ corresponding to the vertical vorticity. The boundary condition is given by a discrete version of eq.(6.1), and then we solve exactly eq.(6.2d), a discretized poisson equation, by using sine transformations.

Numerical simulations are carried out with parameter values: $N = 63$, $\Delta t = 0.1$, $\Delta x = 1.0$, $\eta_1 = 0.6$, $\eta_2 = 0.3$ and $h = -1.0$. The normal rolls should become unstable beyond $R_c = -\eta_2/h$, and the transition to defect chaos is expected because the inequality $g < g_c$ is satisfied. ($g = 10.8$ and $g_c = 18.49$) The initial condition we assumed is a periodic variation in x with small fluctuations. Its wavenumber is $2\pi \times 10/N (= 0.997\cdots)$ and very close to $k_0 = 1$. This choice seems suitable because the roll with wavenumber $k_0 = 1$ shows the fastest initial growth. For $R = 0.5$, we found that the roll solution is stable except that it is slightly deformed near the boundaries. The effect of the boundary seems to be weak compared to isotropic systems. For $R = 1.0$, the roll solution becomes unstable and starts to deform spontaneously and slowly. We can see the formation of defects after the appearance of the zigzag pattern at an early stage. A dynamic steady state is established after a number of creations and annihilations of defects. A time evolution of patterns in the steady state is seen in fig. 3. This shows that the motion and spontaneous creation of defects are the most important ingredients in our pattern dynamics. We identify such a state as defect chaos because the temporal change of the number of defects shows aperiodicity as seen in fig. 3.
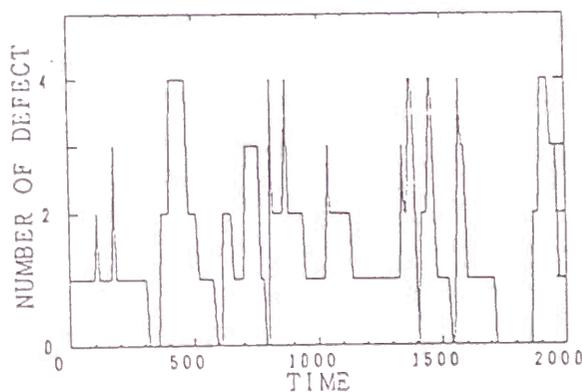

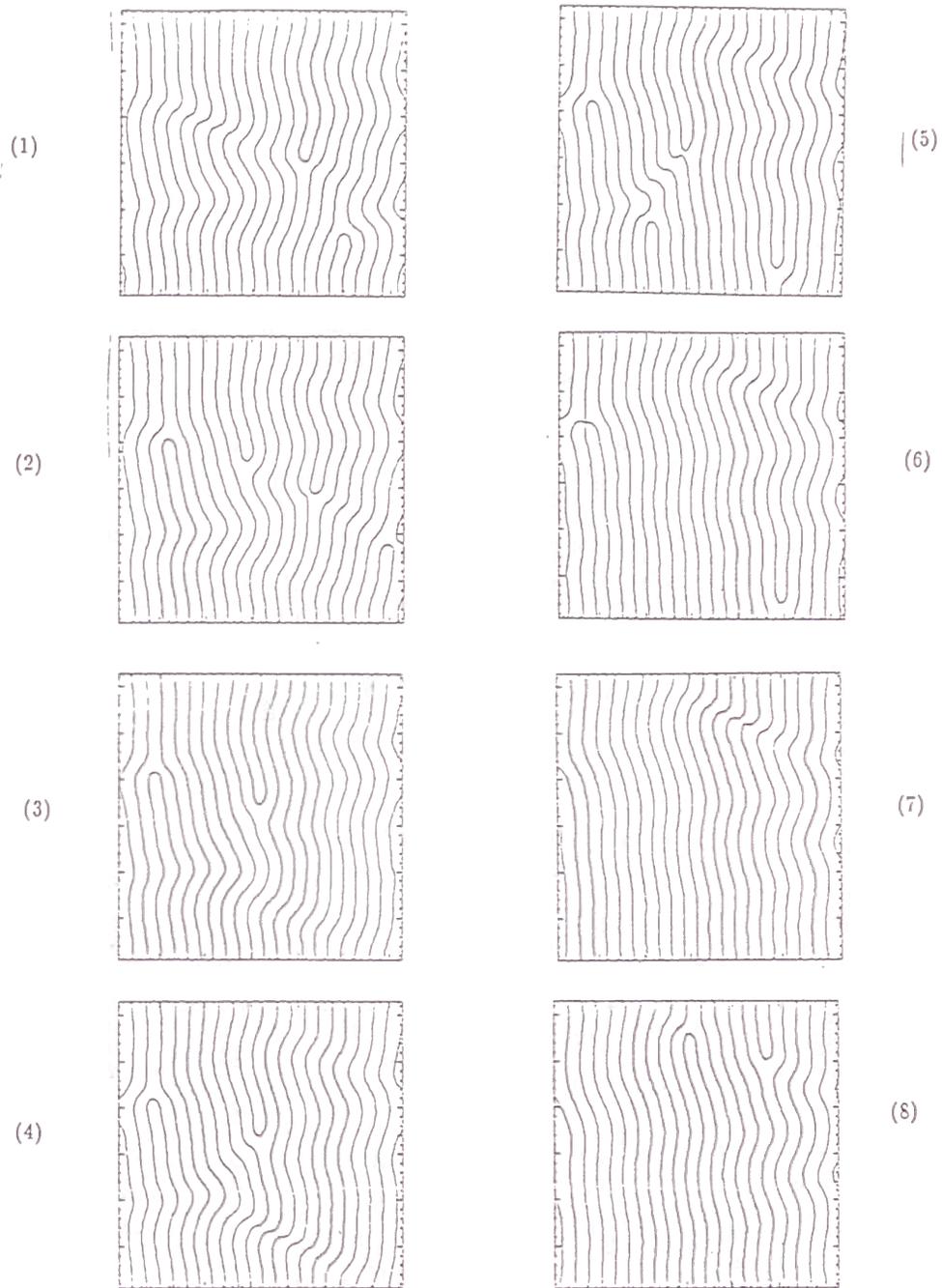Fig.3 Temporal change of the number of defects.

Fig.2 Pattern evolutions at every 100 steps; (1) → (8). The contours $Re(W_s) = 0$, where W_s is interpolated by spline interpolation.

We will now argue some statistical properties of the temporal variation of the number of defects. The quantities $d_n = \sum_{ij} |W_{10n}(i,j)|/N^2$, $(1 \leq n \leq T = 2 \times 10^3)$ for $R = 1.0$ and $R = 1.5$ were calculated. We expected that the low frequency property of the quantity d_n will be identical to that of the number of the defects. In fig. 4, the spectra $S(w)$ of the quantity d_n are shown, where

$$S(w_j) = \left| \frac{1}{T} \sum_{n=1}^{T} d_n e^{2\pi i w_j n} \right|^2,$$

$$w_j = \frac{j}{10 \cdot T}, \qquad (1 \leq j \leq \frac{T}{2} - 1).$$

(6.3)

These spectra seem to have two characteristic regimes:

$$\begin{cases} S(w) \sim const. & \text{for } w \ll w_1; \\ S(w) \sim w^{-\alpha} & \text{for } w_1 \ll w \ll w_2. \end{cases}$$
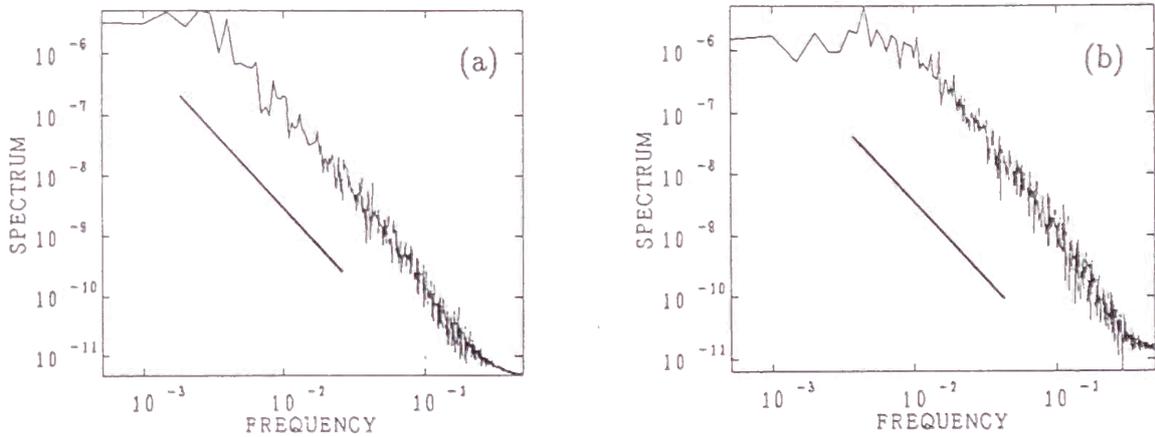
(6.4)

Here $2 < \alpha < 3$ is satisfied.

Fig.4 Log-log plots of spectra $S(w)$ for (a)$R = 1.0$ and (b)$R = 1.5$. These spectra were calculated from the average over five samples. The straight lines show $S(w) \sim w^{5/2}$.

We find further that the cross-over frequency w_1 between the two regimes, which corresponds to the inverse of the correlation time, becomes large with R. This implies that the correlation time diverges at the onset of the zigzag instability. No physical interpretation for these spectral behavior has been presented yet. We still need to investigate their statistical properties in further detail.

7. Concluding Remarks

In the present paper, we investigated analytically and numerically the Pesch-Kramer model supplemented with drift terms, and showed that this model exhibits a transition from stable periodic patterns (WD) to defect chaos (FWD).

In this final section, we will give three comments on (1) the Rayleigh-Bénard convections, (2) an extension to the case of free boundary conditions, and (3) future problems.

(1) Our models can also describe the Rayleigh-Bénard convections when the anisotropic parameters are set as $\eta_1 = \eta_2 = 0$. In that case, the roll solutions do not become unstable because the property $h_{ij} = h > 0$ is always satisfied[55]. On the other hand, experiments and analysis based on the Boussinesq equation show that the rolls become unstable at a finite distant apart from the onset of convection and that the type of the instability at the moderate Prandlt number is the skewed varicose instability[49,69,70]. If we wish to explain *phenomelogically* this fact, the model equation must include more non-linear terms such as $|W|^2 \Delta W$ and $|\nabla W|^2 W$. Indeed, Greenside et al. worked with a modified Swift-Hohenberg equation supplemented with the drift term, and confirmed the transition to a chaotic state[58].

(2) We assumed that the drift field is *adiabatically* induced by the deformations of the rolls. However, if we consider the system under free boundary conditions, the drift flow becomes a relevant dynamical variable by virtue of the Galilei symmetry. Even in the case of rigid boundary conditions, it would be more suitable to start with the case of free boundary conditions as far as the time scale of the drift flows (horizontal time scale) becomes long. In fact, in

the Rayleigh-Bénard convections with low Prandlt number, the breakdown of the Galilei symmetry at the upper and lower plates is weak, and therefore the horizontal time scale is long. In the case of EHC also, Kai et al. showed that the horizontal time scale becomes the same order as the vertical time scale when the frequency of the applied electric fields is relatively high and close to the critical frequency[71]. In these cases, we can expect that the dynamics of the drift becomes relevant.

Recently, Kaiser et al. derived an amplitude equation for EHC under free boundary conditions and showed the direct transition from a convectionless state to defect chaos[72]. We can easily extend our models with the Galilei symmetry and develop the phase dynamics for an extended model. The phase equation takes the form:

$$\dot{\Theta} + \vec{U} \cdot \vec{k} = \sum_{ij} \alpha_{ij}(\vec{k}) \partial_i \partial_j \Theta, \tag{7.1a}$$

$$\dot{U}_i + \vec{U} \cdot \vec{\nabla} U_i = \sum_{lm} d_{lm}(\vec{k}) \partial_{lm} U_i - \sum_{lm} \beta_{ilm}(\vec{k}) \partial_l \partial_m \Theta - \partial_i p, \tag{7.1b}$$

$$\vec{\nabla} \cdot \vec{U} = 0. \tag{7.1c}$$

This equation is an extended version of the phase equation with the Galilei symmetry in essentially one-dimensional systems, where the pressure field was not introduced[73-76].

(3) A number of problems on defect chaos remain to be unsolved, of which the following three are particularly important: The first question is the value of the control parameter R at which the transition to the chaotic state occurs. This question may be related with the problem of spatio-temporal intermittent transition[77-80]. The second problem is how to describe the motions of defects in the defect chaos regime. Although many researches on the defect motions were presented[2-9,81,82], they are concerned with nonchaotic systems. The third problem is to understand the spectral characteristics for the temporal variation of the number of defects. Further reports will be devoted to these subjects.

References

1. N.D. Mermin, Rev.Mod.Phys. **51** 592 (1979).

2. E.D. Siggia and A. Zippelius, Phys.Rev. **A24** 1036 (1981).

3. M.C. Cross, Phys.Rev. **A25** 1065 (1982).

4. Y. Pomeau, S. Zaleski and P. Manneville, Phys.Rev. **A27** 2710 (1983).

5. E.Dubais-Violette, E. Guazzelli and J. Prost, Phil.Mag.**A48** 727 (1983).

6. K. Kawasaki, Prog.Theor.Phys.Suppl. **79** 161 (1984).

7. K. Kawasaki, Prog.Theor.Phys.Suppl. **80** 123 (1984).

8. G. Tesauro and M.C. Cross, Phys.Rev. **A34** 1363 (1986).

9. E. Bodenschatz, W. Pesch and L. Kramer, Physica **D32** 135 (1988).

10. P. Manneville, *Dissipative structures and Weak Turbulence* (Academic Press, New York, 1990)

11. P. Coullet and J. Lega, Europhys.Lett.**7** 511 (1988).

12. P. Coullet, L. Gill, and J. Lega, Phys.Rev.Lett. **62** 1619 (1989).

13. K. Stewartson and J.T. Stuart, J.Fluid Mech. **48** 529 (1971).

14. A.C. Newell, Lectures in Appl.Math. **15** 157 (1974).

15. Y. Kuramoto and T. Tsuzuki, Prog.Theor.Phys. **52** 1399 (1974).

16. Y. Kuramoto, *Chemical Oscillations, Waves, and Turbulence* (Springer, Berlin, 1984)

17. P. Coullet, S. Fauve and E.Tirapegi, J.Phys. (paris), Lett**46** 787 (1985).

18. P. Coullet, C. Elphick, L. Gill and J. Lega, Phys.Rev.Lett. **59** 884 (1987).

19. Y. Kuramoto and S. Koga, Prog.Theor.Phys. **66** 1081 (1981).

20. K. Kaneko, Prog.Theor.Phys. **72** 480 (1984).

21. K. Kaneko, Physica **D34** 1 (1989).

22. K. Kaneko, Physica **D37** 60 (1989).

23. S. Kai and K. Hirakawa, Solid.State.Comm. **18** 1573 (1976).

24. S. Kai and K. Hirakawa, Prog.Theor.Phys.Suppl. **64** 212 (1978).

25. S. Kai, N. Chizumi, and M. Kohno, Phys.Rev. **A40** 6554 (1989).

26. S. Kai and W. Zimmermann, Prog.Theor.Phys.Suppl. **99** 458 (1989).

27. S. Kai, N. Chizumi and M. Kohno, J.Phys.Soc.Jpn. **58** 3541 (1989).

28. A. Joets and R. Ribotta, J.Phys. (paris) **47** 595 (1986).

29. I. Rehberg, S.Rasenat and V. Steinberg, Phys.Rev.Lett. **62** 756 (1989?).

30. S. Nasuno, Dr. thesis, Tohoku University, (1990) (in Japanese).

31. S. Nasuno and S. Kai, *Instabilities and Transition to Defect Turbulence in Electrohydrodynamic Convection of Nematics*, preprint (1990).

32. R. Williams, J.Chem.Phys. **39** 384 (1963).

33. E.F. Carr, Mol.Cryst.Liq.Cryst. **7** 253 (1969).

34. W. Helflich, J.Chem.Phys. **51** 4092 (1969).

35. P.G. de Genne, The Physics of Liquid Crystals (Clarendon, Oxford, England) (1974).

36. A.C. Newell and J. Whitehead, J.Fluid Mech. **38** 279 (1969).

37. L.A. Segel, J.Fluid Mech. **38** 203 (1969).

38. E. Bodenschatz, W. Zimmermann and L. Kramer, J.Phys. (paris) **49** 1875 (1988).

39. W. Pesch and L.Kramer, Z.Phys. **B63** 121 (1986).

40. S. Sasa, Prog.Theor.Phys. **83** 824 (1990).

41. E.D. Siggia and A. Zippelius, Phys.Rev.Lett. **47** 835 (1981).

42. A. Zippelius and E.D. Siggia, Phys.Fluids **26** 2905 (1983).

43. M.C. Cross, Phys.Rev. **A27** 490 (1983).

44. M.C. Cross and A.C. Newell, Physica **10D** 299 (1984).

45. Y. Kuramoto and T. Tsuzuki, Prog.Theor.Phys. **55** 356 (1976).

46. Y. Pomeau and P. Manneville, J.Phys. (paris), Lett**40** 609 (1979).

47. Y. Kuramoto, Prog.Theor.Phys. **71** 1182 (1984).

48. F.H. Busse and R.M. Clever, J.Fluid Mech. **91** 319 (1979).

49. F.H. Busse, Rep.Prog.Phys **41** 1929 (1978).

50. S. Wolfram, Rev.Mod.Phys**55** 601 (1983).

51. Y. Oono and S. Puri, Phys.Rev.Lett. **58** 836 (1987).

52. Y.Oono and S.Puri, Phys.Rev. **A38** 434 (1988).

53. J. Swift and P.C.Hohenberg, Phys.Rev. **A15** 319 (1977).

54. H.S. Greenside and W.M. Coughram Jr., Phys.Rev. **A30** 398 (1984).

55. P. Manneville, J.Phys. (paris), Lett**44** 903 (1983).

56. P. Manneville, J.Phys. (paris) **44** 759 (1983).

57. H.S. Greenside and M.C. Cross, Phys.Rev. **A31** 2492 (1985).

58. H.S. Greenside, M.C. Cross, and W.M. Coughran, Jr, Phys.Rev.Lett. **60** 2269 (1988).

59. S. Sasa, Prog.Theor.Phys. **84** 1008 (1990).

60. A Pocheau, J.Phys. (paris) **50** 2059 (1989).

61. A.C. Newell,T.Passot, and M.Souli, Phys.Rev.Lett. **64** 2378 (1990).

62. Y. Kuramoto, Prog.Theor.Phys.Suppl. **99** 244 (1989).

63. T. Ohta, Prog.Theor.Phys. **73** 1377 (1985).

64. J.S. Langer, Ann.Phys.(N.Y.)**65** 53 (1971).

65. H.P. Brand and R.J. Deissler, Phys.Rev. **A41** 5478 (1990).

66. H.P. Brand and R.J. Deissler, Phys.Rev.Lett. **63** 508 (1989).

67. H. Riecke, Europhys.Lett.**11** 213 (1990).

68. K. Kawasaki and T. Ohta, Physica **116A** 573 (1982).

69. G. Ahlers and D.S. Cannell, Phys.Rev.Lett. **54** 1373 (1985).

70. M.S. Heutmaker and J.P. Gollub, Phys.Rev. **A35** 242 (1987).

71. S. Kai, M. Takada and K. Hirakawa, J.Phys.Soc.Jpn. **45** 2051 (1978).

72. M. Kaiser, W.Pesch and E.Bodenschatz, *Mean Flow Effects in the Electro-Hydrodynamic Convection in Nematic Liquid Crystals* preprint (1990).

73. P. Coullet and S. Fauve, Phys.Rev.Lett. **55** 2857 (1985).

74. U. Frish, Z.S. She and O. Thual, J.Fluid Mech. **168** 221 (1986).

75. B.I. Shraiman, Phys.Rev.Lett. **57** 325 (1986).

76. S. Fauve and E.W. Bolton and M.E. Brachekt, Physica **29D** 202 (1987).

77. K. Kaneko, Prog.Theor.Phys. **74** 1033 (1985).

78. H. Chate and P. Manneville, Phys.Rev.Lett. **58** 112 (1987).

79. H. Chate and P. Manneville, Physica **D32** 402 (1988).

80. S. Ciliberto and P. Bigazzi, Phys.Rev.Lett. **60** 286 (1988).

81. G. Goren, I.Procaccia, S. Rasenat and V. Steinberg, Phys.Rev.Lett. **63**

1237 (1989).

82. S. Nasuno, S. Takeuchi and Y. Sawada, Phys.Rev. **A40** 3457 (1989).